

# Filling ratio of vial

## An important parameter for ball milling

N. Rajabalizadeh Mojarrad<sup>1</sup> · R. Kheirifard<sup>2</sup> · R. Taherzadeh Mousavian<sup>2</sup> · Y. Afkham<sup>2</sup> · S. Nakisa<sup>3</sup>

Received: 26 January 2016 / Accepted: 12 June 2016 / Published online: 1 July 2016  
© Akadémiai Kiadó, Budapest, Hungary 2016

**Abstract** The ratio effect of total volume of balls and powders with respect to volume of vial has not been deeply considered by the researchers for ball milling process. The importance of this new parameter for ball milling process, filling ratio of vial, was investigated in this study. For this purpose, Al-Fe<sub>2</sub>O<sub>3</sub> thermite mixture was used as the starting materials. The powder masses input of 1, 5, 10, and 15 g were loaded into a steel-made vial with 150 cm<sup>3</sup> capacity. Differential scanning calorimetry (DSC), scanning electron microscopy (SEM), X-ray diffraction (XRD), and laser particle size analysis (LPA) were used to evaluate the importance of FRV. The results indicated that by keeping constant all the parameters except FRV, various thermal analysis (DSC) results were obtained, showing the importance of this factor, while the same XRD patterns were revealed. It was found that the main exothermic reaction between Al and Fe<sub>2</sub>O<sub>3</sub> occurred at various temperatures from 940 to 993 °C with various intensities. It was also revealed that for 10 g powder mass input, the reaction mechanism was changed, in which the reactions took place in three steps, before and after the melting of aluminum. The DSC curves were more discussed using SEM and LPA results, focused on morphology of the ball-

milled powders. It was finally suggested that filling ratio of vial should be considered as an important factor in ball milling process.

**Keywords** Filling ratio of vial · Ball milling · DSC · Al-Fe<sub>2</sub>O<sub>3</sub> thermite system

## Introduction

High-energy ball mill (HEBM) is widely used for grinding, alloying, and mechanochemical synthesis of various materials. In this technique, a specified quantity of powder is loaded into a mill vial and processed by interaction (impacts) with balls and by the friction of the balls against each other and the vial's wall [1–8]. This technique can induce chemical reactions between the starting powders that do not normally happen at the room temperature. In fact, HEBM of reactive systems (i.e., mixtures of two or more powders that can react in a self-sustained mode) results in a decrease in the reaction onset temperature and an increase in the reaction rate and intensity [2, 9–11]. However, in order to reduce the required energy for the reactions, the important parameters of HEBM process such as milling time, ball size, milling speed, ball-to-powder mass ratio, and filling ratio of vial (FRV) should be carefully studied and optimized [12–15].

Generally, the importance of FRV is ignored by the researchers, and many articles have not even reported the vial volume [8, 12, 16–21]. This parameter seems to be important especially for mechanochemical synthesis and mechanically activated combustion synthesis processes. A significant decrease in energy transfer from balls to powders could occur when a large number of balls were used or when milling was done at low vial filling levels [1, 22].

✉ R. Taherzadeh Mousavian  
rtaher1898@gmail.com

R. Kheirifard  
ramin.kheirifard@gmail.com

<sup>1</sup> Faculty of Engineering and Natural Sciences, Sabanci University, Istanbul, Turkey

<sup>2</sup> Faculty of Materials Engineering, Sahand University of Technology, Tabriz, Iran

<sup>3</sup> Department of Metallurgy, Zanjan Branch, Islamic Azad University, Zanjan, Iran

If there is not enough space for the balls to freely move inside the vial, the number of collisions between balls increases at the expense of the number of ball–wall collisions, which more efficiently transfers energy to the powder mixture [7].

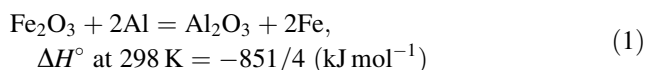
Differential scanning calorimetry (DSC) is a convenient method for investigating chemical thermodynamics and formal kinetic descriptions of physicochemical processes, and many researchers have utilized this technique to study the thermal behavior during milling and combustion synthesis [23–30].

In this study, Al–Fe<sub>2</sub>O<sub>3</sub> thermite system was used to evaluate the effect of FRV on the thermal properties of this mixture. For this purpose, DSC analysis was utilized to compare thermal analysis of the powder mixtures with various powder mass inputs to show whether this parameter is important or not.

## Experimental

The materials used in this study were 99.5 pct pure Al powder and 98.5 pct Fe<sub>2</sub>O<sub>3</sub> powder. The morphology of starting powders is shown in Fig. 1. As can be seen, the average particle size of oxide powders was lower than 1 μm with an almost round shape, while the aluminum particle size was lower than 50 μm in average with irregular shapes.

The powders were mixed with a designed stoichiometry according to Eq. 1, which is a highly exothermic reaction [15].



The powders were then milled for 5 h with a rotating speed of 300 rpm and ball-to-powder weight ratio of 10:1. The milling process was performed under argon atmosphere (with purity of 99.99 %) by using a Fritsch planetary ball mill using steel-made balls (using various balls diameters of 5, 10, 15, and 20 mm, based on the required balls mass) and vial (150 cm<sup>3</sup> capacity). To prevent a significant temperature rise in the mechanically alloyed powders, the 20-min run (milling)–10-min stop (natural cooling) milling cycle was used. The process control agent (PCA) stearic acid with 1.5 mass% of the powders was used to prevent excessive cold welding. By keeping constant the ball milling parameters, various amounts of powder mass input of 1 g (S<sub>1</sub>), 5 g (S<sub>5</sub>), 10 g (S<sub>10</sub>), and 15 g (S<sub>15</sub>) were used to evaluate if this factor could affect the reactions temperature and intensity (heat released during reaction) in Al–Fe<sub>2</sub>O<sub>3</sub> thermite system.

The physicochemical changes for the samples during heating were investigated by a DSC measurement using a Netzsch DSC 404 C (Germany) analyzer to study the effects of FRV on the reaction temperature and intensity.

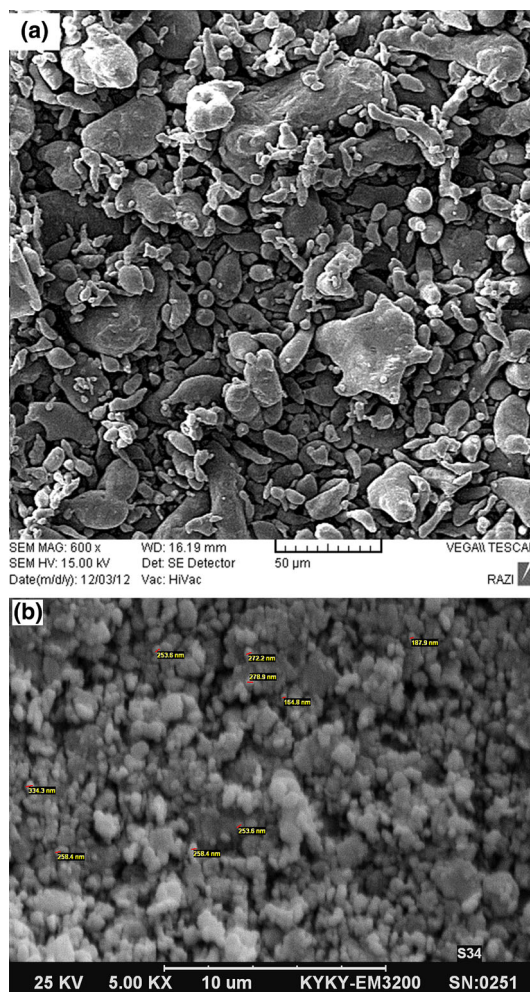


Fig. 1 SEM images of as-received powders, a aluminum, b Fe<sub>2</sub>O<sub>3</sub>

The DSC experiments utilized high-purity corundum as a reference. Powder samples of about 30 mg (30.256, 30.07, 30.696, and 30.112 mg for the samples S<sub>1</sub>, S<sub>5</sub>, S<sub>10</sub>, and S<sub>15</sub>, respectively) were loaded and pressed into an alumina crucible, which will not react with the reactants, and heated up in an inert argon atmosphere at the rate of 10 °C min<sup>-1</sup>. The phase composition of the samples after ball milling was characterized by using X-ray diffractometer (XRD, Bruker's D8 advance system, Germany) using Cu Kα (λ = 0.15405 nm) radiation.

The microstructure of the as-milled samples was studied using two kinds of scanning electron microscopes (SEM, Cam Scan Mv2300 and KYKY-EM3200). Finally, the mean particle size of the powdery samples after ball milling was measured from a laser particle size analyzer (LPA, Malvern, Mastersizer 2000) using distilled water as dispersant in a dispersion unit with the capacity of 150 mL, and the method of wet laser diffraction.

## Results and discussion

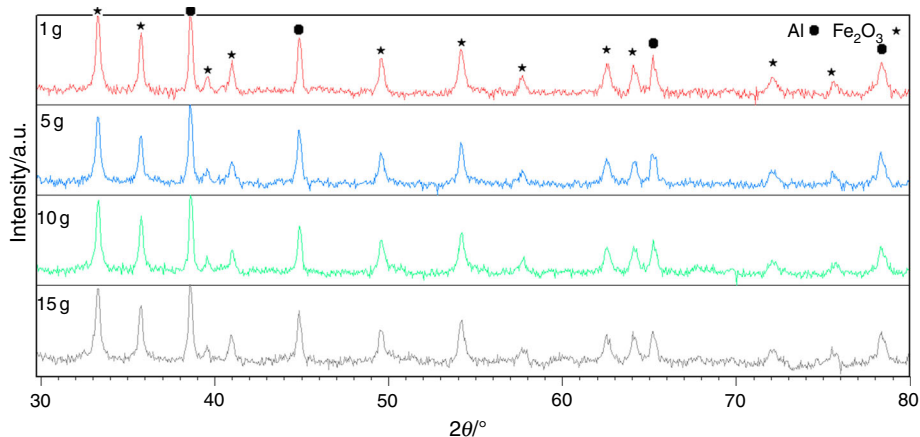
Figure 2 shows the XRD analysis of the ball-milled samples. It could be seen that both the corresponding aluminum and iron oxide ( $\text{Fe}_2\text{O}_3$ ) peaks were revealed, while no other peaks could be detected, showing that no reaction took place after 5 h ball milling for all the samples. It could be observed that almost the same results were obtained for all the samples, indicating that FRV was not effective enough to change the chemical composition of the powders.

Figure 3 shows the SEM microstructures of the milled samples. Figure 3a is related to the sample  $S_1$ , in which 1 g powders as well as 10 g steel balls were loaded in a vial with  $150\text{ cm}^3$  capacity. It has been reported [11, 15] that aluminum ductile powders were flattened as a result of ball collisions, and simultaneously, fine iron oxide particles were distributed on a matrix of aluminum inside the aluminum core and/or on its surface. Therefore, a core-shell superstructure included a core of aluminum with a distribution of fine iron oxide particles and a shell of iron oxide particles was made due to the ball milling of a ductile phase and fine ceramic particles [17]. Figure 4 shows a schematic of core-shell superstructures that were formed after ball milling. A continuous or discontinuous layer of fine ceramic particles formed on the surface of aluminum matrix composite core depended on the amount of fine ceramic particles. For a thermite mixture, the most complete reactions are taken place by a selection of fine metal oxide particles and larger-sized metallic particles [31]. Therefore, an ideal condition for a thermite reaction could be a core of aluminum matrix composite contains a uniform distribution of oxide particles, and a shell of fine oxide particles without any agglomeration on the surface of the core. The corresponding reactions could then occur more completely for such ideal core-shell superstructure

during prolonged ball milling or after combustion synthesis. Figure 3a–d more or less shows the same morphology, in which fine oxide particles were present on the surface of composite powders (based on the EDAX analysis). However, it could be seen that by changing the FRV, the particle size of the powders was changed, in which more larger particles were detected for samples  $S_5$  (see Fig. 3b) and  $S_{15}$  (see Fig. 3d), while Fig. 3c shows lower-sized composite particles for the sample  $S_{10}$ . However, LPA characterization was required to justify the SEM results.

Figure 5a–d shows LPA results of the samples, milled with various amounts of powder mass inputs. It could be seen that arithmetic mean diameter (AMD,  $\mu\text{m}$ ) for the sample  $S_{10}$  was the lowest, while samples  $S_{15}$  and  $S_5$  have a highest value of AMD. It could be also observed that the geometric mean diameter (GMD,  $\mu\text{m}$ ) of the sample  $S_{10}$  is minimum compared with those of the other samples. These results confirmed the SEM results, in which lower-sized composite powders were obtained for the sample  $S_{10}$ . It can be concluded that FRV could affect the morphology and particle size of ball-milled powders. It is important to note that two maximum peaks were observed for the samples  $S_{10}$  and  $S_{15}$ , in which higher mass inputs were loaded, while the two other samples have just one maximum peak. It could be observed that the height of first maximum peak for sample  $S_{10}$  is higher than that of the second maximum peak. In fact, by increasing the powder mass input, heavier balls were used that caused an incorporation of higher mechanical energy to the powders. Therefore, a higher work hardening amount could be observed for the powders that led to a more fragmentation and formation of submicron particles. However, for the sample  $S_{15}$ , the high volume of the powders and balls led to collisions that were more inefficient. The balls velocity was not high enough during rotating, as lower free space was present in the vial. Therefore, the formation of lower-sized composite powders

**Fig. 2** X-ray phase analysis of the ball-milled samples



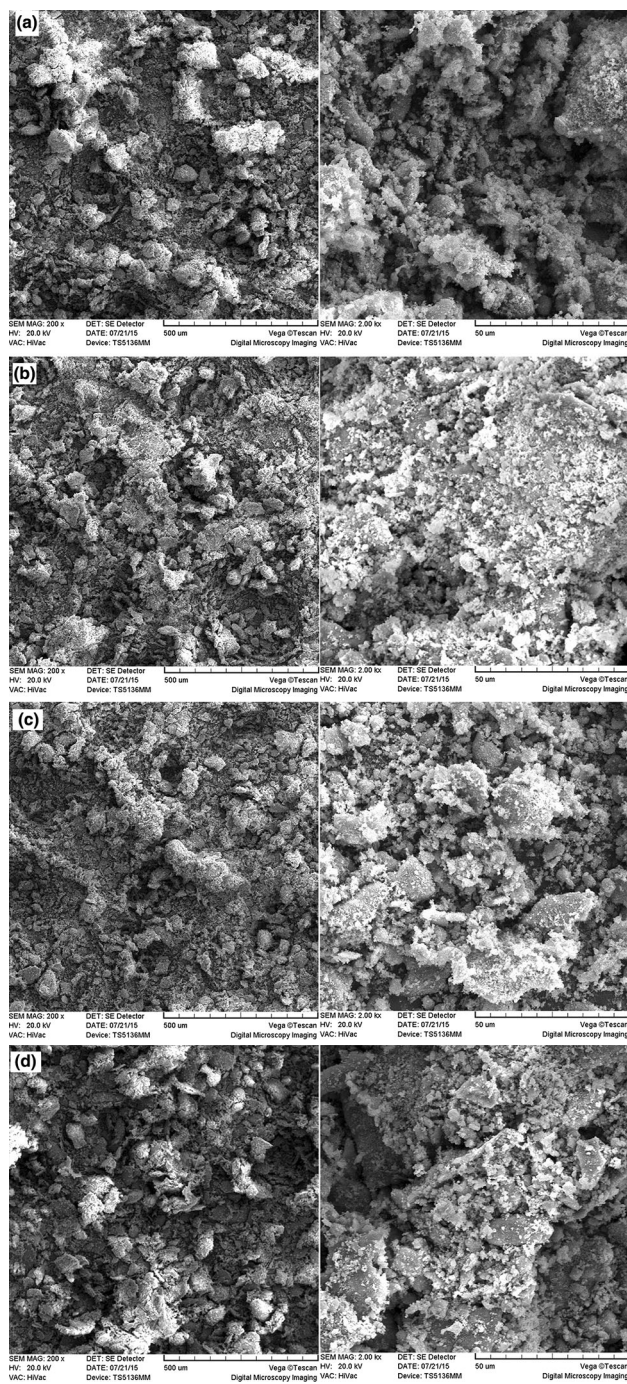


**Fig. 3** SEM images of the ball-milled samples  $S_1$  (a),  $S_5$  (b),  $S_{10}$  (c), and  $S_{15}$  (d)

with core–shell superstructures is directly depended on the work hardening and effective ball-to-powder collisions.

As mentioned, the main importance of FRV factor could be found via thermal analysis and DSC measurements. Figure 6 shows the thermal analysis of the samples. As can be seen, considerable difference in thermal behavior of the samples was revealed, showing that FRV was highly effective on the amount of milling-induced mechanical energy

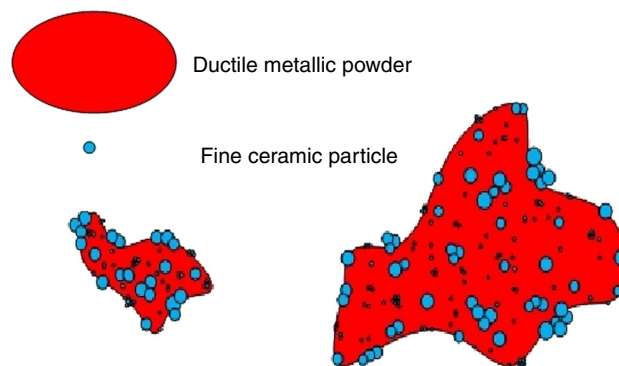


**Fig. 4** Schematic of core–shell superstructures after ball milling of ductile metallic powders and fine ceramic particles

that entered into the powders. It could be observed that endothermic peaks, which are related to the melting of aluminum, were revealed at about 640–680 °C for all the samples. This figure shows that all the samples experienced a liquid-state exothermic reaction at a range of 900–1000 °C, in which exothermic peaks were detected for the samples  $S_{10}$  and  $S_{15}$  at lower temperatures below 950 °C. As reported in the literature [9, 11], the main role of mechanical activation process is to reduce the exothermic reactions temperature and to increase their intensities that by increasing the milling time and rotation speed, the required exothermic reactions for combustion synthesis occurred at lower temperatures with higher intensities. More than 50 °C reduction in reaction temperature was obtained in this study (see Fig. 6) without changing the milling time and speed, just by changing the FRV factor.

The other point that could be found from Fig. 6 is the change of reaction mechanism for the sample  $S_{10}$ . As can be seen, the combustion synthesis was occurred at three stages for this sample. The first step took place before the aluminum melting in the solid state, while our previous studies [9, 11, 15] showed such occurrence due to mechanical activation process. The second exothermic reaction was formed just after the melting of aluminum, and the main reaction occurred at about 944 °C. Therefore, it seems that there was a higher tendency for reaction between the milled powders of sample  $S_{10}$  at lower temperatures, while the other samples did not reveal such tendency, showing that FRV even affect the reaction mechanism for Al– $Fe_2O_3$  thermite mixture.

It is also interesting to note that the reaction occurred for the sample  $S_5$  at about 990 °C. The SEM and LPA results showed the formation of more agglomerated large-sized composite powders for this sample. In fact, effective interfacial areas would be decreased if agglomeration occurs. Therefore, higher time and temperature are required for such thermite mixture to reveal exothermic reactions. On the other hand, the reaction occurs more

**Fig. 5** LPA results of ball-milled samples  $S_1$  (a),  $S_5$  (b),  $S_{10}$  (c), and  $S_{15}$  (d)

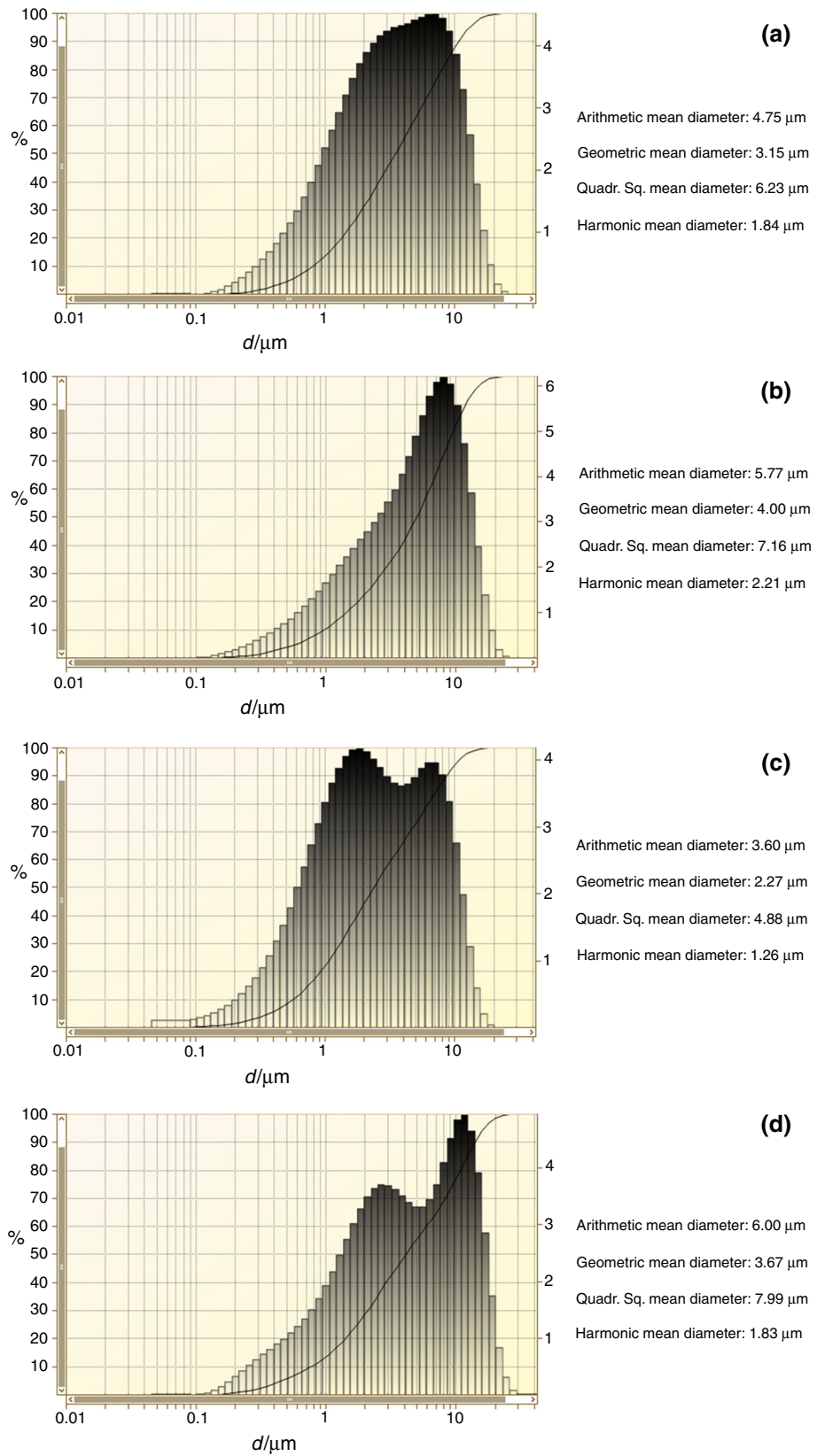


**Fig. 6** DSC analysis results of the ball-milled powdery samples

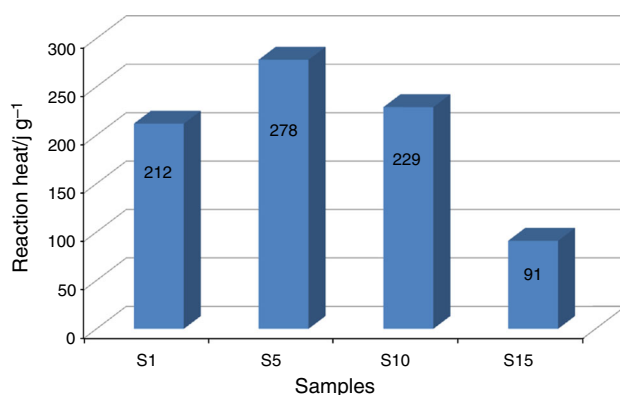
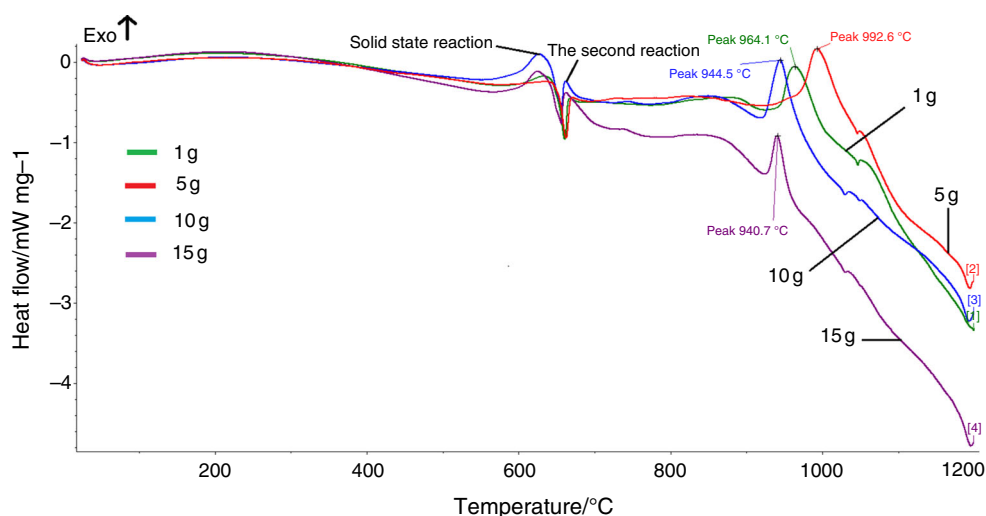


**Fig. 7** Measured values of reaction heat for the last exothermic peaks, obtained from DSC analysis

intensively for this sample ( $S_5$ ), showing that higher mechanical energy might be introduced into this sample. Although the same reaction temperatures were obtained for the samples  $S_{10}$  and  $S_{15}$ , lower reaction intensity was obtained for the sample  $S_{15}$ . In fact, a combination of thermodynamic- and kinetic-induced reasons affects the thermal analysis of the powders. The simultaneous formation of effective interfacial areas between the starting powders and effective ball-to-powder collisions might lead to the occurrence of more intensive exothermic reactions at lower temperatures. It could be observed that the main exothermic reaction took place for the sample  $S_{10}$  at a lower temperature, while its intensity was considerable.

By calculation of the integrated area under an exothermic peak and based on the heating rate during DSC measurements, heat of reaction (enthalpy) could be determined. Figure 7 shows the measured reaction heats of the last exothermic reaction (known as the main reaction), which clearly indicates the sharp reduction in enthalpy for the sample  $S_{15}$  as a result of inefficient collisions. As can be

seen, samples  $S_5$  and  $S_{10}$  have the highest amounts of reaction heat, respectively. Two parameters must be considered for obtaining the highest values of reaction enthalpy: first, occurrence of effective ball-to-powder collisions to increase the efficiency of ball milling and avoid the reduction in balls velocity, and second, using of heavy balls to guarantee the required entrance of mechanical energy into the powders. Figure 7 shows the higher importance of the effective collisions rather than using heavy balls as sample  $S_1$  with light balls has a considerable amount of reaction heat, while sample  $S_{15}$  has a very low value of reaction enthalpy. Based on the DSC results obtained for the samples  $S_5$  and  $S_{10}$ , it could be deduced that the ideal powder mass input for a vial with  $150 \text{ cm}^3$  capacity might be in the range of 5–10 g to achieve the lowest reaction temperature and highest intensity.

Based on the obtained results, it can be suggested that FRV should be considered as an important effective parameter in ball milling process.

## Conclusions

In this study, the effect of FRV was studied on the thermal behavior of Al– $\text{Fe}_2\text{O}_3$  thermite mixture using DSC analysis to show the importance of this parameter. From the experimental results, the followings were drawn:

1. The various amount of powder mass input could not affect the XRD results of the ball-milled powders.
2. Based on the SEM microstructures, a core of aluminum matrix composite contains a distribution of oxide particles, and a shell of fine oxide particles was obtained after ball milling. However, it was revealed that various composite powder particle sizes were obtained by changing the powder mass input.

3. LPA results confirmed the SEM results in the case of powder mass input effect on the morphology and particle size. It was found that by using 5 g (sample S<sub>5</sub>) and 15 g (sample S<sub>15</sub>) mass input, the maximum particle sizes were obtained as SEM characterization exactly showed more agglomerated particles for the samples S<sub>5</sub> and S<sub>15</sub>. The minimum particle size was obtained for the sample S<sub>10</sub>, in which 10 g powders were loaded.
4. DSC analysis showed the importance of FRV. It was obtained that FRV is a very important parameter that affects the thermal behavior of ball-milled powders. It was found that for a vial with 150 cm<sup>3</sup> capacity, 5–10 g mass input range could lead to the best results in the case of reaction temperature and intensity.

## References

1. Suryanarayana C. Mechanical alloying and milling. *Prog Mater Sci.* 2001;46(1):1–184.
2. Kuziora P, Wyszynska M, Polanski M, Bystrzycki J. Why the ball to powder ratio (BPR) is insufficient for describing the mechanical ball milling process. *Int J Hydrog Energy.* 2014;39(18):9883–7.
3. Mousavian RT, Sharafi S, Shariat M. Preparation of nano-structural Al<sub>2</sub>O<sub>3</sub>-TiB<sub>2</sub> in situ composite using mechanically activated combustion synthesis followed by intensive milling. *Iran J Mater Sci Eng.* 2011;8(2):1–9.
4. Suryanarayana C, Ivanov E, Boldyrev V. The science and technology of mechanical alloying. *Mater Sci Eng A.* 2001;304:151–8.
5. Benjamin J. Fundamentals of mechanical alloying. *Mater Sci Forum.* 1992;88:1–18.
6. Bernoosi S, Azari Khosroshahi R, Taherzadeh Mousavian R. Mechanical properties of hot-pressed Al-4.5 wt% Cu/WC composite. *J Ultrafine Grained Nanostruct Mater.* 2014;47(2):63–70.
7. Gotor F, Achimovicova M, Real C, Balaz P. Influence of the milling parameters on the mechanical work intensity in planetary mills. *Powder Technol.* 2013;233:1–7.
8. Forouzan M, Mousavian RT, Sharif T, Afkham Y. A three-step synthesis process of submicron boron carbide powders using microwave energy. *J Therm Anal Calorim.* 2015;122(2):579–88.
9. Mousavian RT, Sharafi S, Roshan M, Shariat M. Effect of mechanical activation of reagents' mixture on the high-temperature synthesis of Al<sub>2</sub>O<sub>3</sub>-TiB<sub>2</sub> composite powder. *J Therm Anal Calorim.* 2011;104(3):1063–70.
10. Rogachev A, Moskovskikh D, Nepapushev A, Sviridova T, Vadchenko S, Rogachev S, et al. Experimental investigation of milling regimes in planetary ball mill and their influence on structure and reactivity of gasless powder exothermic mixtures. *Powder Technol.* 2015;274:44–52.
11. Mousavian RT, Sharafi S, Shariat M. Microwave-assisted combustion synthesis in a mechanically activated Al-TiO<sub>2</sub>-H<sub>3</sub>BO<sub>3</sub> system. *Int J Refract Met Hard Mater.* 2011;29(2):281–8.
12. Farhanchi M, Neysari M, Barenji RV, Heidarzadeh A, Mousavian RT. Mechanical activation process for self-propagation high-temperature synthesis of ceramic-based composites. *J Therm Anal Calorim.* 2015;122(1):123–33.
13. Razavi-Tousi S, Szpunar J. Effect of ball size on steady state of aluminum powder and efficiency of impacts during milling. *Powder Technol.* 2015;284:149–58.
14. Mosleh A, Ehteshamzadeh M, Mousavian RT. Fabrication of an r-Al<sub>2</sub>Ti intermetallic matrix composite reinforced with  $\alpha$ -Al<sub>2</sub>O<sub>3</sub> ceramic by discontinuous mechanical milling for thermite reaction. *Int J Miner Metall Mater.* 2014;21(10):1037–43.
15. Mousavian RT, Azizi N, Jiang Z, Boostani AF. Effect of Fe<sub>2</sub>O<sub>3</sub> as an accelerator on the reaction mechanism of Al-TiO<sub>2</sub> nanothermite system. *J Therm Anal Calorim.* 2014;117(2):711–9.
16. Boostani AF, Mousavian RT, Tahamtan S, Yazdani S, Khosroshahi RA, Wei D, et al. Graphene sheets encapsulating SiC nanoparticles: a roadmap towards enhancing tensile ductility of metal matrix composites. *Mater Sci Eng A.* 2015;648:92–103.
17. Mousavian RT, Khosroshahi RA, Yazdani S, Brabazon D, Boostani AF. Fabrication of aluminum matrix composites reinforced with nano-to micrometer-sized SiC particles. *Mater Des.* 2016;89:58–70.
18. Boostani AF, Tahamtan S, Jiang Z, Wei D, Yazdani S, Khosroshahi RA, et al. Enhanced tensile properties of aluminium matrix composites reinforced with graphene encapsulated SiC nanoparticles. *Compos A Appl Sci Manuf.* 2015;68:155–63.
19. Raju KSR, Raju VR, Raju PRM, Ghosal P. Investigation of novel parameters affecting distribution of reinforcement in nano metal matrix composites. *Int J Nanomanuf.* 2015;11(1–2):94–109.
20. Boostani AF, Yazdani S, Mousavian RT, Tahamtan S, Khosroshahi RA, Wei D, et al. Strengthening mechanisms of graphene sheets in aluminium matrix nanocomposites. *Mater Des.* 2015;88:983–9.
21. Raju KSR, Raju VR, Raju PRM, Ghosal P. Launching particle to constant reinforcement ratio as a parameter for improving the nanoreinforcement distribution and tensile strength of aluminum nanometal matrix composites. Paper presented at “International conference on advances in design & manufacturing” (ICAD&M14), 5–7 Dec 2014, National Institute of Technology, Tiruchirappalli, Tamil Nadu, India. *Int J Mater Res.* 2015.
22. Suryanarayana C, Al-Aqeeli N. Mechanically alloyed nanocomposites. *Prog Mater Sci.* 2013;58(4):383–502.
23. Zhu H, Dong K, Wang H, Huang J, Li J, Xie Z. Reaction mechanisms of the TiC/Fe composite fabricated by exothermic dispersion from Fe-Ti-C element system. *Powder Technol.* 2013;246:456–61.
24. Azzaza S, Alleg S, Suñol J-J. Microstructure characterization and thermal stability of the ball milled iron powders. *J Therm Anal Calorim.* 2015;119(2):1037–46.
25. Lysenko E, Surzhikov A, Vlasov V, Malyshev A, Nikolaev E. Thermal analysis study of solid-phase synthesis of zinc- and titanium-substituted lithium ferrites from mechanically activated reagents. *J Therm Anal Calorim.* 2015;122(3):1347–53.
26. Lin H-L, Zhang G-C, Lin S-Y. Real-time co-crystal screening and formation between indomethacin and saccharin via DSC analytical technique or DSC-FTIR microspectroscopy. *J Therm Anal Calorim.* 2014;120(1):679–87.
27. Liu G, Hu J. The thermal behavior of alumina borate whisker with Bi(OH)<sub>3</sub>-Sn(OH)<sub>4</sub> coatings. *Powder Technol.* 2012;218:124–30.
28. Sina H, Iyengar S. Reactive synthesis and characterization of titanium aluminides produced from elemental powder mixtures. *J Therm Anal Calorim.* 2015;122(2):689–98.
29. Bharvada E, Shah V, Misra M. Exploring mixing uniformity of a pharmaceutical blend in a high shear mixture granulator using enthalpy values obtained from DSC. *Powder Technol.* 2015;276:103–11.
30. Stoia M, Muntean C, Militaru B. Fine MnFe<sub>2</sub>O<sub>4</sub> nanoparticles for potential environmental applications. *J Therm Anal Calorim.* 2015;121(3):1003–10.
31. Weismiller M, Malchi J, Lee J, Yetter R, Foley T. Effects of fuel and oxidizer particle dimensions on the propagation of aluminum containing thermites. *Proc Combust Inst.* 2011;33(2):1989–96.